

# Soft-Switching Auxiliary Current Control for Improving Load Transient Response of Buck Converter

Doogwook Kim, Joonho Shin, and Jong-Won Shin  
 School of Energy Systems Engineering, Chung-Ang University

## ABSTRACT

A control technique for the auxiliary buck/boost converter is proposed herein to improve the load transient response of the buck converter. The proposed technique improves the system efficiency by enabling the soft switching operation of the auxiliary converter. The design guidelines for achieving capacitor charge balance for the output capacitor during the transient are also presented herein. The experimental results revealed that the output voltage undershoot and settling time during the load step-up transient were 40 mV and 14  $\mu$ s, respectively, and the output voltage overshoot and settling time during the load step-down transient were 35 mV and 21  $\mu$ s, respectively. The performance and effectiveness of the proposed technique were experimentally verified using a prototype buck converter with a 15-V input, 3.3-V output, and 200-kHz switching frequency.

## 1. Introduction

Various control techniques have previously been developed to improve the load transient response of the buck converter. The time-optimal control based on the capacitor charge balance (CCB) enables minimum output voltage fluctuation without the aid of auxiliary circuits<sup>[1]</sup>. Previous studies have emphasized the simple implementation and operation of resistive auxiliary circuits<sup>[2]-[3]</sup>. The auxiliary switched resistor attenuates the output voltage fluctuation, reduce the efficiency, and increase the electromagnetic interference (EMI) caused by the high di/dt of the switches<sup>[2]</sup>. The auxiliary inductor and bidirectional switches require complicated control circuits and impose a heavy computational burden on the digital integrated circuit (IC)<sup>[3]</sup>. Additionally, the resistance in the freewheeling path degrades the efficiency.

Control techniques employing nonresistive auxiliary circuits can also improve the dynamic response<sup>[4]-[6]</sup>. The auxiliary inductor exploits the resonance and soft switching<sup>[4]</sup>, but the auxiliary switches must be controlled differently and according to whether the load is stepped up or down, which increases the controller complexity. The high-frequency switching controllers of the auxiliary circuit have been described in previous papers<sup>[5]-[6]</sup>. The average current of the auxiliary inductor has been controlled to a constant value to achieve CCB during the load transient<sup>[5]</sup>. Adaptive slope control has also been

proposed to further improve the load transient response<sup>[6]</sup>. However, these control techniques require high-bandwidth sensors and high-speed digital ICs, which increase the controller complexity.

This paper proposed a technique for peak-current-controlling the auxiliary current in critical conduction mode (CRM). The technique minimizes the output voltage deviation during the load transient through cycle-by-cycle CCM, while the soft turn-on of the auxiliary switches suppresses the efficiency degradation and EMI generation. The remainder of this paper is organized as follows; Section 2 describes the circuit operation and design conducted via the proposed control scheme. The experimental results are presented in Section 3, and the conclusions are presented in Section 4.

## 2. Proposed Control Technique

### 2.1 Implementation of proposed control circuit

Fig. 1 shows the main converter ( $Q_1$ ,  $Q_2$ , and  $L_1$ ) and auxiliary buck/boost converter ( $Q_3$ ,  $Q_4$ , and  $L_2$ ) connected in parallel. The literals  $V_{in}$ ,  $v_o$ ,  $i_{L1}$ ,  $i_{L2}$ , and  $i_o$  denote the input voltage, output voltage, main inductor current, auxiliary inductor current, and load current, respectively. The voltages  $v_{gsi}$  and  $v_{dsi}$  denote the gate-source and drain-source voltages of the metal-oxide-semiconductor field-effect transistor (MOSFET)  $Q_i$ , respectively. In the steady state,  $Q_3$  and  $Q_4$  are turned off, while  $Q_1$  and  $Q_2$  are operational via the conventional voltage mode controller (VMC). During the load transient,  $Q_3$  and  $Q_4$  operate along with  $Q_1$  and  $Q_2$  to control  $i_{L2}$  and improve the transient response.

The key waveform of the proposed auxiliary current control is shown in Fig. 2. The literals  $V_{ref}$  and  $\Delta I_o$  are the target output voltage and magnitude of the  $i_o$  variation, respectively. During the transient period caused by stepping up  $i_o$  and  $t_1$ - $t_5$ ,  $Q_1$  is fully turned on while  $Q_2$  is

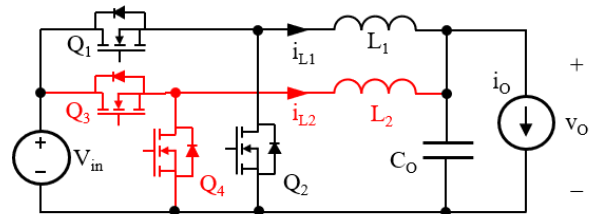


Fig. 1. Main buck converter ( $Q_1$ ,  $Q_2$ , and  $L_1$ ) and auxiliary buck/boost converter ( $Q_3$ ,  $Q_4$ , and  $L_2$ ) for applying proposed auxiliary current control.

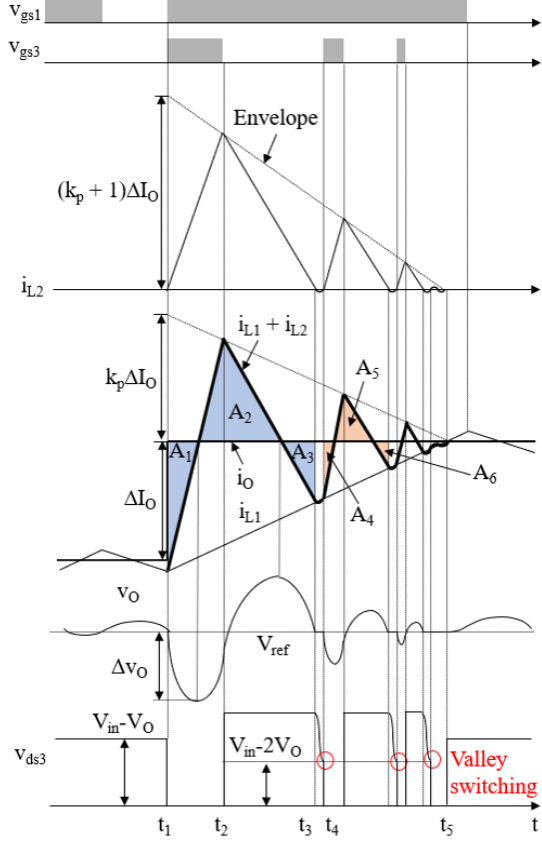


Fig. 2. Key waveforms of proposed auxiliary current control when  $i_o$  is stepped up ( $N=3$ ).

fully turned off shown in Fig. 2. The auxiliary converter works as a peak-current-mode-controlled buck converter in the CRM. Switch  $Q_3$  operates as the main switch of the auxiliary buck converter to produce the triangular wave shapes of  $i_{L2}$  under an envelope. The first switching period of the auxiliary converter comprises three switching states:

- State 1 [ $t_1-t_2$ ]: Current  $i_o$  is stepped up at  $t_1$ ;  $Q_3$  turns on, and  $i_{L2}$  increases linearly.
- State 2 [ $t_2-t_3$ ]: When  $i_{L2}$  reaches the envelope at  $t_2$ ,  $Q_3$  turns off, and  $i_{L2}$  decreases and freewheels through the body diode of  $Q_4$ . Switch  $Q_4$  can be ON as a synchronous rectifier to reduce the conduction loss.
- State 3 [ $t_3-t_4$ ]: When  $i_{L2}$  reaches zero at  $t_3$ , the output parasitic capacitances of  $Q_3$  and  $Q_4$  and  $L_2$  resonate. Switch  $Q_3$  turns on again at  $t_4$ , when  $v_{ds3}$  is minimum. During this state, the  $v_o$  variation is assumed to be negligible.

These states are repeated  $N$  times before the steady-state operation resumes and VMC regains control at  $t_5$ . The number  $N$  can be limited to avoid the risk of excessively high switching frequencies and power losses. The switching loss of  $Q_3$  is minimized via valley switching, that is, by  $Q_3$  turning on at the valley of  $v_{ds3}$ . Switch  $Q_3$  may turn on with zero-voltage switching (ZVS) if  $V_{in} \leq 2v_o$ .

Area  $A_n$  represents the amount of charge that is charged to or discharged from the output capacitor  $C_o$ , to which the  $v_o$  deviation is proportional. The coefficient  $k_p$  is set to

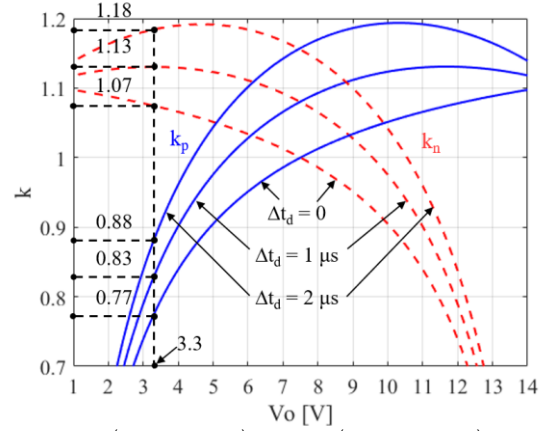


Fig. 3.  $k_p$  (solid curves) and  $k_n$  (dotted curves) versus  $v_o$  under conditions defined in Table 1.

Table 1. Circuit parameters of experiment.

Parameter	Description
$V_{in}$	15 V
$v_o$	3.3 V
$i_o$	4 A–15 A
Switching frequency of $Q_1$ and $Q_2$	200 kHz
$L_1$	10 $\mu$ H
$L_2$	500 nH
$C_o$	220 $\mu$ F

maintain the CCB of  $C_o$  in each switching cycle, as expressed in (1).

$$A_i + A_{i+2} = A_{i+1} \quad (i=1,4,7,\dots) \quad (1)$$

Section 2.2 presents the derivation of  $k_p$  in detail. The undershoot of  $v_o$ ,  $\Delta v_o$ , is the function of voltages, inductances, and  $\Delta I_o$  and is solely determined by  $A_1$ , as expressed in (2).

$$\Delta v_o = \frac{A_1}{C_o} = \frac{\Delta I_o^2 L_1 L_2}{2C_o(L_1 + L_2)(V_{in} - V_o)} \quad (2)$$

When  $i_o$  is stepped down, the auxiliary converter operates as a peak-current-mode-controlled boost converter in CRM. Switch  $Q_4$  acts as the main switch of the auxiliary boost converter and turns on with ZVS if  $V_{in} > 2v_o$ , while  $Q_1$  is fully off and  $Q_2$  is fully on.

## 2.2 Envelope for Capacitor-Charge-Balance

The magnitude of  $i_{L2}$  is controlled by the envelope of which height is  $(k_p + 1)\Delta I_o$  as shown in Fig. 2. The constant  $k_p$  is a function of  $V_{in}$ ,  $V_o$ ,  $L_1$ , and  $L_2$  and is independent from  $\Delta I_o$ , as expressed in (3).

$$k_p = \frac{L_1 V_o - L_2 (V_{in} - 2V_o)}{L_1 V_o + L_2 (V_{in} - 2V_o)} \quad (3)$$

The other constant  $k_n$  that determines the envelope when  $i_o$  is stepped down can be obtained using (4).

$$k_n = \frac{L_1 (V_{in} - V_o) + L_2 (V_{in} - 2V_o)}{L_1 (V_{in} - V_o) - L_2 (V_{in} - 2V_o)} \quad (4)$$

In practical implementation, the first turn-on of  $Q_3$  may be delayed by the time  $\Delta t_d$  from the step change of  $i_o$ . Fig. 3 plots  $k_p$  and  $k_n$  versus  $v_o$  when  $V_{in}$ ,  $L_1$ ,  $L_2$ , and  $I_o$  are as presented in Table 1. The plots are symmetric with respect

to the  $V_O = V_{in}/2$  line (7.5 V in this paper) when  $\Delta t_d=0$ , because the increasing and decreasing slope of  $i_{L1}+i_{L2}$  are interchanged between the step-up and step-down cases of  $i_o$ . The nonzero  $\Delta t_d$  increases both  $k_p$  and  $k_n$ .

### 3. Experimental Verification

The prototype circuit shown in Fig. 1 was built; its parameters are listed in Table 1. The VMC control loop had a  $78.6^\circ$  phase margin at the 12-kHz cutoff frequency via a PIC type-3 compensator and the control circuit was configured by analog ICs only. Fig. 4 shows the experimental waveform of  $i_o$  (magenta trace),  $i_{L1}+i_{L2}$  (red),  $v_o$  (blue),  $v_{ds3}$  and  $v_{ds4}$  (green) of the proposed control scheme when  $i_o$  was stepped up and down, respectively. The delay  $\Delta t_d$  was  $1.2 \mu\text{s}$  at step-up and  $0.5 \mu\text{s}$  at step-down. In Fig. 4(a), The measured undershoot voltage and settling time were 40 mV and  $14 \mu\text{s}$ , respectively. As can be seen,  $Q_3$  valley-switched to reduce the switching loss and noise. In Fig. 4(b), the measured overshoot voltage and settling time were 35 mV and  $21 \mu\text{s}$ , respectively. The  $Q_4$  was zero-voltage-switched, reducing switching loss and noise during the load step-down transient.

### 4. Conclusion

An auxiliary current control technique is proposed herein to improve the load transient response of buck converter. The proposed scheme controls the auxiliary buck/boost converter through the peak current mode in CRM. The proposed control scheme minimizes the output voltage deviation and power loss of the auxiliary circuit via soft-switching auxiliary switches. Experimental results by 15 V-3.3 V, 200-kHz buck converter demonstrated the improved dynamic response: the undershoot was 40 mV and the settling time was  $14 \mu\text{s}$  when the output current was stepped from 4 A to 15 A, and the overshoot was 35

mV and settling time was  $21 \mu\text{s}$  when the output current was stepped from 15 A to 4 A.

This research was supported by Energy Cloud R&D Program through the National Research Foundation of Korea(NRF) funded by the Ministry of Science, ICT (2019M3F2A1073313).

### References

- [1] E. Meyer, Z. Zhang, and Y. F. Liu, "An optimal control method for buck converters using a practical capacitor charge balance technique," *IEEE Trans. Power Electron.*, vol. 23, no. 4, pp. 1802-1812, Jul. 2008.
- [2] S. Kapat, P. S. Shenoy, and P. T. Krein, "Near-null response to large-signal transients in an augmented buck converter: a geometric approach," *IEEE Trans. Power Electron.*, vol. 27, no. 7, pp. 3319-3329, Jul. 2012.
- [3] W. Lu, Z. Zhao, Y. Ruan, S. Li, and H. H. C. Iu, "Two-period frame transient switching control for buck converter using coupled-inductor auxiliary circuit," *IEEE Trans. Ind. Electron.*, vol. 66, no. 10, pp. 8040-8050, Oct. 2019.
- [4] Z. Shan, S. C. Tan, C. K. Tse, and J. Jatskevich, "Augmented buck converter design using resonant circuits for fast transient recovery," *IEEE Trans. Power Electron.*, vol. 31, no. 8, pp. 5666-5679, Aug. 2016.
- [5] E. Meyer, Z. Zhang, and Y. F. Liu, "Controlled auxiliary circuit to improve the unloading transient response of buck converters," *IEEE Trans. Power Electron.*, vol. 25, no. 4, pp. 806-819, Apr. 2010.
- [6] Y. Wen and O. Trescases, "DC-DC converter with digital adaptive slope control in auxiliary phase for optimal transient response and improved efficiency," *IEEE Trans. Power Electron.*, vol. 27, no. 7, pp. 3396-3409, Jul. 2012.

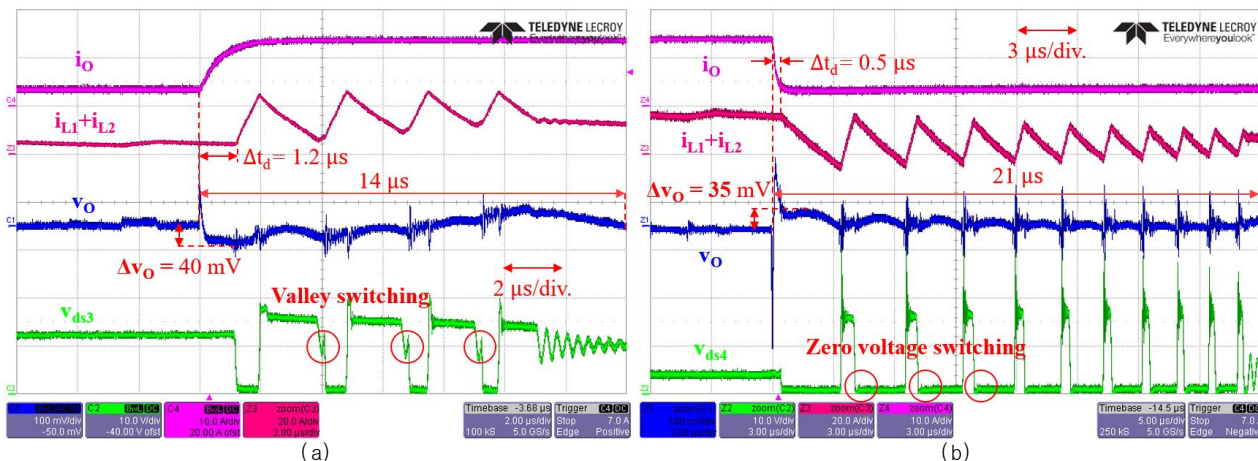


Fig. 4. Experimental waveforms of proposed control technique; trace  $i_o$  (magenta) is in 10 A/div; trace  $i_{L1} + i_{L2}$  (red) is in 20 A/div; trace  $v_o$  (blue) is in 100 mV/div. with AC coupling; trace  $v_{ds3}$  or  $v_{ds4}$  (green) are in 10 V/div. (a) When  $i_o$  is stepped up from 4 to 15 A with  $N = 4$ ; time scale is  $2 \mu\text{s/div}$ . (b) When  $i_o$  is stepped down from 15 to 4 A with  $N = 10$ ; time scale is  $3 \mu\text{s/div}$ .